Critical Hysteresis in a Tilted Washboard Potential

M. Borromeo
Dipartimento di Fisica and Istituto Nazionale di Fisica Nucleare, Università di Perugia, I-06100 Perugia, Italy

G. Costantini
Istituto Nazionale di Fisica della Materia, Università di Camerino, I-62032 Camerino, Italy

F. Marchesoni
Istituto Nazionale di Fisica della Materia, Università di Camerino, I-62032 Camerino, Italy, and Department of Physics, University of Michigan, Ann Arbor, Michigan 48109-1120

(Received 10 August 1998)

The Brownian motion in a tilted washboard potential subjected to a low-frequency periodic drive develops large hysteresis loops, which attain their maximum at the locked-to-running transition in the underdamped regime. The dependence of such a critical phenomenon on the drive parameters and on the temperature is investigated numerically. Moreover, this hysteresis mechanism is related to the occurrence of random multiple jumps, whose length and time duration distributions appear to decay according to a universal power law with exponent $\alpha = 1.5$. This model may explain various instances of low-frequency excess damping in material science. [S0031-9007(99)08872-9]

PACS numbers: 05.40.Jc, 05.20.Dd, 05.60.Cd, 82.20.Db

The classical Brownian motion in a washboard potential has been investigated to a great extent in connection with a variety of condensed phase phenomena, such as Josephson junction currents [1], superionic conduction [2], dielectric relaxation [3], plasma physics [4], surface diffusion [5], and polymer dynamics [6], to mention but a few. The most comprehensive review on this topic is to be found in Risken's textbook [7], where the diffusion in a washboard potential is analyzed within the framework of the Fokker-Planck formalism. Lately, a surge of interest [8–10] was kindled by the debate on the characterization and physics significance of the so-called multiple jumps, or flights, when an underdamped Brownian particle jumps over many a potential barrier before getting trapped again (see also Risken's unstationary solutions [7]). Eventually, the extension of the Fokker-Planck formalism to spatially periodic systems (eigenvalue-band analysis [10], dynamic structure factor approach [9]) proved capable of reproducing quite closely the flight statistics reported in recent simulation studies [8].

In this Letter we take on the ultimate challenge posed in Risken's textbook, namely, the question of hysteresis in a periodically driven *tilted* potential at low damping. Such a phenomenon becomes apparent at the locked-to-running transition, which is known to occur for weak static tilts (proportional to the damping constant). The relevant hysteresis loops are the largest for certain values of the forcing frequency and the temperature. Moreover, we observed that the multiple jump statistics changes dramatically in the presence of a low-frequency periodic drive, no matter how small its amplitude: The flight length and time duration distributions seem to decay according to a universal power law, independent of the forcing frequency and the particle temperature. Furthermore, hysteresis induces an additional contribution to the internal friction that opposes the driving periodic modulation [11]: In the present model of Brownian motion the excess damping turns out to diverge at vanishingly low frequencies, in suggestive analogy with the internal friction in various materials and devices.

The Brownian motion in a tilted washboard potential is fully described by the stochastic differential equation (in rescaled units [7])

$$\ddot{x} = -\gamma\dot{x} - \omega_0^2 \sin x + F + \xi(t), \tag{1}$$

where the force terms on the right-hand side represent, respectively, a viscous damping with constant γ, a spatially periodic, tilted substrate described by the potential

$$V(x, F) = \omega_0^2(1 - \cos x) - Fx, \tag{2}$$

and a stationary zero mean-valued, Gaussian noise with autocorrelation function $\langle \xi(t)\xi(0)\rangle = 2\gamma kT\delta(t)$.

The time evolution of the stochastic process $x(t)$ is characterized by random switches between a *locked* state with zero average velocity and a *running* state with asymptotic average velocity $\langle v\rangle = \langle \dot{x}\rangle = F/\gamma$. In terms of the mobility $\mu(F) \equiv \langle v\rangle/F$ the locked and running state correspond to $\gamma\mu = 0$ and $\gamma\mu = 1$, respectively. In the noiseless case $\xi(t) \equiv 0$, the average speed of the Brownian particle depends on the initial conditions according to a static hysteresis loop [7]: In the *underdamped* regime $\gamma \ll \omega_0$, the transition from the locked to the running state occurs when increasing F above $F_3 = \omega_0^2$, while the opposite transition takes place on lowering F below $F_1 = (4/\pi)\gamma\omega_0$. Of course, for sufficiently large values of γ, say, in the *damped* regime with $\gamma > (\pi/4)\omega_0$, the distinction between F_1 and F_3

 0031-9007/99/82(14)/2820(4)$15.00

is meaningless; the locked-to-running transition is located at $F = F_3$, no matter what the initial conditions.

The weak noise case, or zero temperature limit $T = 0+$, brings about a totally different scenario, where the *stationary* dynamics of $x(t)$ is controlled by a single threshold $F_2 \simeq (2 + \sqrt{2})\gamma\omega_0$: For $F < F_2$ the Brownian particle gets trapped in one potential well; for $F > F_2$ it falls down the tilted periodic substrate with average speed F/γ. At the threshold F_2 the quantity $\gamma\mu(F)$ jumps from zero up to one stepwise. For finite but low temperatures, $kT \ll \omega_0^2$, the locked-to-running transition is continuous, but still confined within a narrow neighborhood at about F_2 (Fig. 1). The critical behavior of $\gamma\mu(F)$ in the vicinity of the transition threshold is the signature of a strongly nonlinear system response and involves long relaxation times [7].

In order to shed light on the mechanism responsible for the locked-to-running transition, we replaced the static tilt F in Eq. (1) with

$$F(t) = F_0 + \Delta F \cos(\Omega t + \varphi)\,. \tag{3}$$

Here, the sinusoidal component of $F(t)$ is treated as a perturbation with $\Delta F \ll F_0$, while its initial phase φ can be set to zero without loss of generality.

The most evident effect of the time periodic drive in Eq. (3) is the appearance of hysteresis loops in the parametric curves of the steady state average velocity $\langle v(F)\rangle$ or, equivalently, of the mobility $\mu(F)$ versus F (Fig. 1). For forcing periods $T_\Omega = 2\pi/\Omega$ larger than the intrawell resonance period $2\pi/\omega_0$, the mobility hysteresis loops are $2\Delta F$ wide, centered on the static mobility curve $\mu(F_0)$ and traversed in the counterclockwise direction; with increasing T_Ω their major axis approaches the tangent to the curve $\mu(F_0)$; for the phase lag between $F(t)$ and the system response $\langle v(t)\rangle$ decreases from π down to zero (Fig. 1a). Hysteresis loops have been observed even for values of T_Ω much larger than the relevant Kramers time $\tau_K \sim (kT/2\omega_0^2\gamma)\exp(2\omega_0^2/kT)$ [12], the longest relaxation time scale in the stationary process (1).

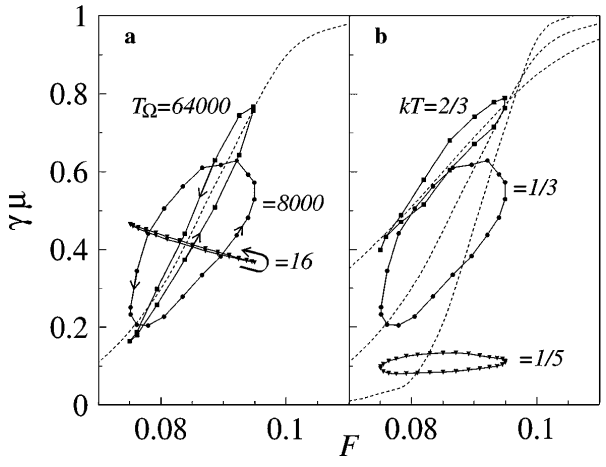

FIG. 1. Oriented hysteresis loops for the mobility $\mu(F)$ at different values of the forcing period with $kT = 1/3$ (a) and different values of kT with $T_\Omega = 8 \times 10^3$ (b). In both panels $F_0 = 0.085$ and $\Delta F = 0.01$; the dashed curves represent $\gamma\mu(F)$ as obtained numerically in the absence of periodic forcing for $\gamma = 0.03$ and $\omega_0 = 1$. Points on loops are equally spaced in time.

The main properties of the hysteresis phenomenon thus revealed are displayed graphically in Figs. 1–3.

(i) Criticality.—The phenomenon attains its maximum for values of F_0 comprised within the transition jump width of the curve $\mu(F_0)$; more precisely, the optimal choice of F_0 seems to be given by the condition that $\gamma\mu(F_0) = 1/2$. Figure 1b shows indirectly the *critical* nature of this hysteresis mechanism. For values of F_0 relatively far from F_2 no appreciable hysteresis loops were detected. Moreover, the area encircled by these loops grows quadratically with the amplitude ΔF of the periodic drive, as expected [7].

(ii) Frequency dependence.—In order to characterize the frequency dependence of the phenomenon at hand we plotted the area $A(\Omega)$ encircled by the velocity hysteresis loops and the corresponding average power $P(\Omega)$ dissipated by the periodic drive (3) versus the angular frequency Ω (see Figs. 2a and 2b). The quantities $A(\Omega)$ and $P(\Omega)$ are easily related to the first coefficients of the Fourier series expansion of $\langle v(t)\rangle$, namely,

$$A(\Omega) = -\oint \langle v(t)\rangle dF = \pi\Delta F v_s(\Omega)\,, \tag{4}$$

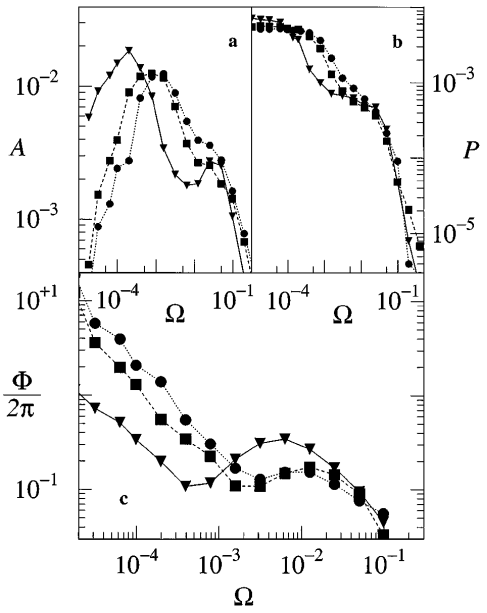

FIG. 2. Frequency dependence of the velocity hysteresis loop area $A(\Omega)$ (a) and average power $P(\Omega)$ dissipated by the periodic drive (b) for different values of the temperature. The ratio $P(\Omega)/A(\Omega)$ is the internal friction $\Phi(\Omega)/2\pi$ per defect plotted in (c) (see text). In (a)–(c), F_0 is chosen to coincide with the optimal choice $\gamma\mu(F_0) = 0.5$, namely, $F_0 = 0.086$ at $kT = 1/4$ (triangles); $F_0 = 0.085$ at $kT = 1/3$ (squares); $F_0 = 0.090$ at $kT = 2/5$ (circles). Other simulation parameters are $\Delta F = 0.01$, $\gamma = 0.03$, and $\omega_0 = 1$.

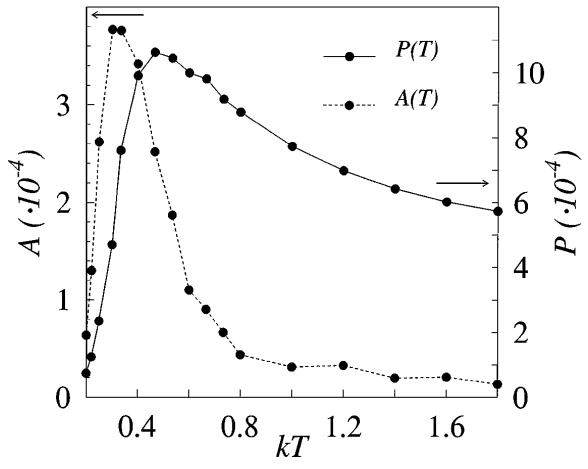

FIG. 3. Hysteresis loop area A and average dissipated power P versus temperature for $T_\Omega = 8 \times 10^3$ and $F_0 = 0.085$. Other simulation parameters are $\Delta F = 0.01$, $\gamma = 0.03$, and $\omega_0 = 1$.

$$P(\Omega) = \frac{\Delta F}{T_\Omega} \int_0^{T_\Omega} \langle v(t) \rangle \cos(\Omega t) dt = \frac{\Delta F}{2} v_c(\Omega), \quad (5)$$

where

$$v_c(\Omega) = \frac{2}{T_\Omega} \int_{-T_\Omega/2}^{T_\Omega/2} \langle v(t) \rangle \cos(\Omega t) dt,$$

$$v_s(\Omega) = \frac{2}{T_\Omega} \int_{-T_\Omega/2}^{T_\Omega/2} \langle v(t) \rangle \sin(\Omega t) dt. \quad (6)$$

The curves $A(\Omega)$ exhibit a main peak in correspondence with the interwell hopping rate $\Omega \sim \tau_K^{-1}$ [12], and a side peak, attributable to the intrawell relaxation process for $\Omega \sim \gamma$, that shoots up from the background only at low temperatures. In the limit of Ω tending to zero, $A(\Omega)$ vanishes proportional to Ω, while $P(\Omega)$ increases up to a plateau; hence, at low frequencies $\Omega < \tau_K^{-1}$, the average dissipated power is frequency independent. The different low-frequency behaviors of $A(\Omega)$ and $P(\Omega)$ are discussed at a later time.

(iii) Temperature dependence.—The temperature dependence of the critical hysteresis phenomenon was investigated by keeping the parameters of the time dependent tilt $F(t)$ (F_0, Ω, and ΔF) fixed and by varying the temperature. For instance, in Fig. 3 the static tilt F_0 was chosen so as to satisfy the optimal condition $\gamma \mu(F_0) = 1/2$ at $kT/\omega_0^2 = 1/3$ and then kT was varied without further tuning F_0. The loop area $A(T)$ and the average dissipated power $P(T)$ peak at different values of the temperature, closely resembling the stochastic resonance phenomenon [13]. The reason why $A(T)$ peaks at $kT/\omega_0^2 = 1/3$ is a consequence of the critical nature of the hysteresis mechanism under study (see also Fig. 1b): On changing kT, the choice of the static tilt F_0 is no longer optimal and thus the relevant hysteresis loop shrinks. The quantity $P(T)$ peaks at a higher temperature and is a more reliable signature of stochastic resonance [14,15].

Critical hysteresis in a tilted washboard potential has interesting consequences on the statistics of the multiple jumps that are known to occur in the underdamped regime [8–10]. Figure 4 summarizes well the conclusions of our simulation work: Under the action of a low-frequency periodic drive, the flight lengths and time durations are distributed according to a *universal* power law.

In the absence of periodic drive $\Delta F = 0$, we explored the static tilt range from below F_1 up to above F_2: For no value of F_0 we managed to detect flight length (or time duration) distributions with nonexponential tails. In close agreement with the predictions of Ref. [9], our distributions show a fast drop for relatively short flights, followed by a slower exponential decay with time constant of the order of τ_K for the longest flights (see inset of Fig. 4) [16].

In the presence of a low-frequency periodic drive, $\Omega < \tau_K^{-1}$, we distributed the flights recorded during each cycle according to their length X and time duration T_x, thus obtaining the relevant distributions $N(X)$ and $N(T_x)$. For the sake of comparison, we then rescaled T_x into an effective length X_t by multiplying the flight time duration T_x times the asymptotic speed F_0/γ of the *running state*, $X_t = (F_0/\gamma)T_x$. In Fig. 4 the two distributions $N(X)$ and $N(X_t)$ are compared: They appear to overlap even if, for the parameter values of the simulations, $\langle v \rangle = F_0/2\gamma$. This means that the Brownian particle performs multiple jumps with average speed F_0/γ and *very small dispersion*.

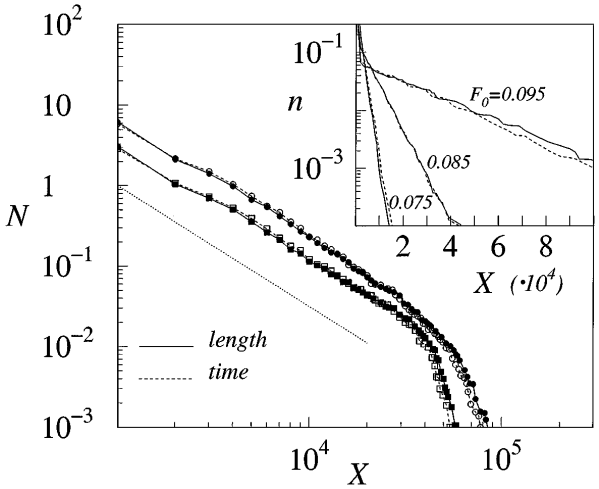

FIG. 4. Distribution of the number of flights per forcing cycle according to length and time duration (in length units, see text) for $T_\Omega = 3.2 \times 10^4$ (squares) and $T_\Omega = 6.4 \times 10^4$ (circles). The power law $N(X) \sim X^{-\alpha}$ with $\alpha = 1.5$ is drawn for reader's convenience (dotted straight line). Inset: Flight number density with respect to length and time duration in the absence of periodic forcing for different values of F_0 close to F_2. Other simulation parameters are $\Delta F = 0.01$, $\gamma = 0.03$, and $\omega_0 = 1$.

Figure 4 clearly shows that (a) the integrals of $N(X)$ and $N(X_t)$, i.e., the average number of flights per forcing cycle, are proportional to T_Ω. As a consequence, the number density of flights per unit of time is *independent* of the forcing frequency, and (b) $N(X)$ and $N(X_t)$ decay like power laws with exponent $\alpha \simeq 1.5$ independent of Ω (and the temperature). Of course, it fails for time durations longer than a half forcing period, as the sign reversal of the periodic drive becomes important (finite size effect). The flight distributions are correlated in phase with the periodic drive. Most of the longest flights take place during the half-cycle when $\Delta F \cos(\Omega t)$ is positive. This explains the different behavior of $A(\Omega)$ and $P(\Omega)$ for $\Omega \to 0$ in Figs. 2a and 2b: The correlation between $\langle v(t) \rangle$ and $\Delta F \cos(\Omega t)$ increases with decreasing Ω, so that $v_c(\Omega)$ [and $P(\Omega)$] approach a plateau, while $v_s(\Omega)$ [and $A(\Omega)$] vanish.

The notion of critical hysteresis has a potential application to many problems in material science. For instance, it may be invoked to explain the low-frequency *excess* damping observed in metals [17,18]. In this case, the pointlike Brownian defect of Eq. (1) must be replaced by a sine-Gordon string [19] that models the dislocation dynamics on a lattice periodic substrate; the string center of mass can be easily shown to undergo critical hysteresis. Furthermore, it has been known since the 1960s that a dislocation network should be envisaged as a metastable system arranged into relatively large domains, each subjected to a random *subcritical* internal stress (Pare's model [11]). In a real internal friction experiment, such an internal stress combines with the externally applied periodic stress, in perfect analogy with the time dependent tilt (3) of our model. The details of a hysteretic model of low-frequency dislocation damping will be reported in a forthcoming publication.

[1] V. Ambegaokar and B. I. Halperin, Phys. Rev. Lett. **22**, 1364 (1969).

[2] P. Fulde, L. Pietronero, W. R. Schneider, and S. Strässler, Phys. Rev. Lett. **35**, 1776 (1975).

[3] J. R. McConnel, *Rotational Brownian Motion and Dielectric Theory* (Academic, London, 1980).

[4] E. M. Lifshitz and L. P. Pitaevskii, *Physical Kinetics* (Pergamon, Oxford, 1981), Chap. 3; T. Katsouleas and J. Dawson, Phys. Rev. Lett. **51**, 392 (1983).

[5] R. Ferrando, R. Spadacini, and G. E. Tommei, Phys. Rev. E **48**, 2437 (1993).

[6] G. I. Nixon and G. W. Slater, Phys. Rev. E **53**, 4969 (1996).

[7] H. Risken, *The Fokker-Planck Equation* (Springer, Berlin, 1984), Chap. 11.

[8] E. Pollak, J. Bader, B. J. Berne, and P. Talkner, Phys. Rev. Lett. **70**, 3299 (1993).

[9] R. Ferrando, R. Spadacini, and G. E. Tommei, Phys. Rev. E **51**, 126 (1995).

[10] P. Jung and B. J. Berne, in *New Trends in Kramers' Theory*, edited by P. Talkner and P. Hänggi (Kluwer, Dordrecht, 1995), p. 67.

[11] A. S. Nowick and B. S. Berry, *Anelastic Relaxation in Crystalline Solids* (Academic, New York, 1972).

[12] R. Ferrando, R. Spadacini, and G. E. Tommei, Phys. Rev. A **46**, R699 (1992); P. Talkner and E. Pollak, Phys. Rev. E **47**, R21 (1993).

[13] L. Gammaitoni, P. Hänggi, P. Jung, and F. Marchesoni, Rev. Mod. Phys. **70**, 223 (1998).

[14] F. Marchesoni, Phys. Lett. A **231**, 61 (1997).

[15] Note that, in view of Eqs. (4) and (5) and Fig. 2, the amplitude of the fundamental periodic component of $\langle v(t) \rangle$ with frequency Ω, $v(\Omega, T) = \sqrt{v_c(\Omega, T)^2 + v_s(\Omega, T)^2}$, is quantitatively dominated by $v_c(\Omega, T)$. The amplitude $v(\Omega, T)$ turns out to be a monotonic decaying function of Ω and a resonant function of T.

[16] We are aware of possible ambiguities as to how to determine the end point of a flight [9]: Locking after each flight was required explicitly in our numerical code.

[17] F. Marchesoni and M. Patriarca, Phys. Rev. Lett. **72**, 4101 (1994).

[18] G. Cagnoli *et al.*, Phys. Lett. A **213**, 245 (1996), and references therein.

[19] C. Cattuto and F. Marchesoni, Phys. Rev. Lett. **79**, 5070 (1997).